ORIGINAL SCIENTIFIC PAPER

CROATICA CHEMICA ACTA

Croat. Chem. Acta **2025**, *98*(4), 279–287
Published online: January 14, 2026
DOI: 10.5562/cca4224

HKD 1926

Synthesis, Characterization and Biological Evaluation of Imidazo[1,2-*a*]pyridine Integrated Thiazole Chalcones as Potent Anti-Breast Cancer and Antimicrobial Agents

Samadhan A. Shenmare,[1,2] Dnyaneshwar M. Sirsat,[3] Sadanand N. Shringare,[1] Nagesh V. Edake,[1] Nikita N. Mali,[4] Raghunath B. Bhosale,[1] Pravin S. Bhale[2,*]

[1] Organic Chemistry Research Laboratory, School of Chemical Sciences, Punyashlok Ahilyadevi Holkar Solapur University, Solapur-413255, Maharashtra, India
[2] Department of Chemistry, Yeshwantrao Chavan Mahavidyalaya, Tuljapur, Dist-Dharashiv-413601, Maharashtra, India
[3] Department of Chemistry, Anandibai Raorane Arts, Commerce & Science College, Vaibhavwadi, Dist-Sindhudurg-416 810, Maharashtra, India
[4] Department of Chemistry, Sub-Campus, Dr. Babasaheb Ambedkar Marathwada University, Dharashiv-413 501, Maharashtra, India
* Corresponding author's e-mail address: bhale.ps@gmail.com

RECEIVED: November 01, 2025 ✶ REVISED: November 25, 2025 ✶ ACCEPTED: December 02, 2025

Abstract: A novel series of imidazo[1,2-*a*]pyridine–thiazole–chalcone hybrids (**8a**–**l**) were synthesized and evaluated for their in vitro anticancer and antimicrobial activities. The anticancer potential was assessed against the human breast cancer cell line MCF-7 using the sulforhodamine B (SRB) assay. Most of the synthesized compounds exhibited moderate cytotoxic activity, with compound **8i** showing the highest potency (GI_{50} = 19.0 μM) compared to the reference drug adriamycin (GI_{50} = 0.4 μM). Structure–activity relationship (SAR) analysis revealed that electron-donating substituents, particularly methoxy groups at the para-position of the phenyl ring in the thiazole moiety, significantly enhanced anticancer activity, whereas electron-withdrawing groups such as cyano reduced it. The antimicrobial efficacy of the synthesized derivatives were determined by the disc diffusion method against bacteria. Several compounds, notably **8g**, **8j**, **8k**, and **8l** exhibited broad-spectrum antimicrobial activity comparable to the standard drug ciprofloxacin. Overall, these findings demonstrate that imidazo[1,2-*a*] pyridine–thiazole–chalcone hybrids represent a promising class of multifunctional bioactive molecules with significant anticancer and antimicrobial potential, offering valuable insights for future structural optimization and therapeutic development.

Keywords: imidazo[1,2-*a*] pyridine, thiazole, anti-cancer activity, antimicrobial activity.

INTRODUCTION

ACCORDING to the World Health Organization (WHO), cancer remains one of the leading causes of mortality worldwide, accounting for nearly 10 million deaths in 2020.[1] The WHO further estimated that approximately 20 million new cancer cases and 9.7 million deaths occurred globally in 2022, with projections indicating a 77 % increase in new cases by 2050. Statistical analyses revealed that lung (12.6 %), breast (11.6 %), and colorectal (9.6 %) cancers were the first, second, and third most commonly diagnosed malignancies in 2022, respectively.

In terms of mortality, lung cancer accounted for the highest proportion of cancer-related deaths (18.7 %), followed by colorectal (9.3 %), liver (7.8 %), and breast cancers (6.9 %). These findings underscore the substantial and growing global health burden posed by cancer.[2] Breast cancer is a complex and diverse malignancy that arises from the uncontrolled growth of epithelial cells within breast tissue. Advancements in early diagnostic techniques and therapeutic interventions have markedly improved patient survival outcomes, however, breast cancer stands as the most commonly diagnosed carcinoma and remains the primary cause of cancer-related fatalities among women worldwide.[3,4] These challenges emphasize

the urgent need for the development of novel chemotherapeutic agents with greater specificity and enhanced therapeutic efficacy.

In this regard, molecular hybridization has emerged as a powerful strategy that enables the combination of two pharmacologically active moieties within a single molecular framework, thereby allowing simultaneous modulation of multiple biological targets.[5] This approach offers promising solutions to major limitations of conventional chemotherapy.

Imidazo[1,2-*a*]pyridine derivatives have attracted significant attention in recent years owing to their unique fused heterocyclic structure and broad spectrum of biological activities. The imidazo[1,2-*a*]pyridine scaffold has emerged as a valuable framework in drug discovery due to its ability to interact with various biological targets and its structural adaptability for pharmacophore modification. Compounds bearing the imidazo[1,2-*a*]pyridine core exhibit a wide range of pharmacological activities, including antiulcer, anticonvulsant, antiprotozoal, anthelmintic, antiepileptic, antifungal, antibacterial, analgesic, antiviral, anticancer, anti-inflammatory, antitubercular, and antitumor properties.[6–8] Owing to this remarkable biological versatility, the imidazo[1,2-*a*]pyridine-based derivative GSK461364A (Figure 1) serves as a potent and selective inhibitor of Polo-like kinase 1 (PLK1), effectively disrupting mitotic progression and inducing cell-cycle arrest. This compound has demonstrated significant anticancer potential across multiple tumor models, primarily through PLK1 inhibition–mediated apoptotic pathways.[9]

In recent years, numerous imidazo[1,2-*a*]pyridine-based compounds have been identified as promising anticancer agents. Notably, derivatives bearing substituents at the C2 and C3 positions of the imidazo[1,2-*a*]pyridine scaffold have demonstrated particularly potent anticancer activity.[10,11]

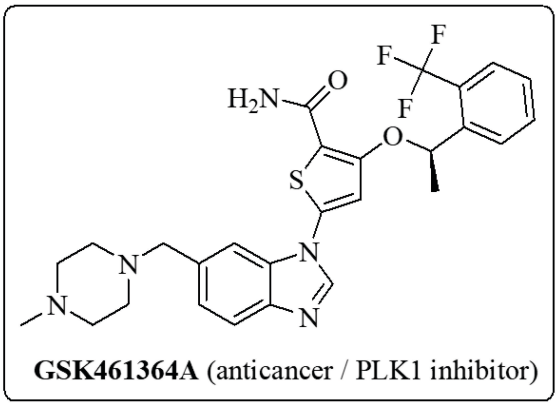

Figure 1. Imidazo[1,2-*a*]pyridine-based derivative GSK461364A.

On the other side, thiazole is a valuable pharmacophore with broad pharmaceutical relevance, as its derivatives exhibit diverse biological activities, including antioxidant, antibacterial, anticancer, anti-inflammatory, and antifungal properties.[12,13] The thiazole scaffold is present in over 18 FDA-approved drugs, such as cefiderocol (Fetroja®, 2019) for multidrug-resistant Gram-negative infections, alpelisib (Piqray®, 2019) for breast cancer, lusutrombopag (2018) for thrombocytopenia, and cobicistat (2018) for HIV therapy.[14–18] These examples highlight the thiazole nucleus as a privileged scaffold in modern drug design.

Over the past few decades, molecular hybridization has emerged as a powerful strategy in medicinal chemistry for designing hybrid molecules with enhanced biological activity through the combination of two or more pharmacophores or bioactive scaffolds. This approach offers a promising means to overcome key limitations of existing therapeutics, such as poor selectivity, limited specificity, and the development of multidrug resistance, particularly in anticancer drug design. In our previous studies, we have reported several biologically active molecular hybrids with significant anticancer potential.[19–24] Building upon these findings and continuing our efforts toward the development of novel bioactive anticancer agents,[25–29] we have synthesized a new series of imidazo[1,2-*a*]pyridine–thiazole–chalcone hybrids (**8a–l**) and subsequently evaluated their in vitro anticancer and antimicrobial activities.

EXPERIMENTAL

Materials and Methods

All chemicals used in the synthesis were of synthetic grade and obtained from commercial suppliers. The progress of reactions was monitored by thin-layer chromatography (TLC) on silica gel 60 F254 aluminum-backed plates (Merck). TLC spots were visualized under UV light and/or iodine vapors. All solvents were dried using suitable drying agents prior to use. Melting points were determined by the open-end capillary method and are uncorrected. ^{1}H NMR spectra were recorded in $CDCl_3$ on a Bruker AV-400 MHz spectrometer, and ^{13}C NMR spectra were obtained at 75 MHz. Chemical shifts (δ, ppm) were referenced to tetramethylsilane (TMS) as an internal standard. IR spectra were recorded on a Shimadzu FT-IR spectrophotometer using 1 % potassium bromide (KBr) pellets. Mass spectra were obtained on a Shimadzu LCMS-2010EV instrument (Shimadzu, Japan). Anticancer activity assays were performed at the Tata Memorial Centre, Advanced Centre for Treatment, Research, and Education in Cancer (ACTREC), Kharghar, Navi Mumbai–410210.

Synthesis

General procedure for the preparation of imidazo[1,2-*a*] pyridine integrated thiazole chalcones (8a-l):

Thiazole ketone 3a–c (5.0 mmol) was dissolved in ethanol (15 mL), and the corresponding imidazo[1,2-*a*]pyridine-3-carbaldehyde 7a–d (5.0 mmol) was added, followed by the addition of a 10 % aqueous sodium hydroxide solution. The reaction mixture was stirred at room temperature for 24 h. After completion of the reaction, as confirmed by thin-layer chromatography (TLC), the mixture was cooled to room temperature. The resulting precipitate was collected by filtration and recrystallized from ethanol to afford the pure yellow solid product (**8a–l**).

SPECTRAL DATA OF REPRESENTATIVE COMPOUNDS

(2*E*)-3-(2-(4-fluorophenyl)-*H*-imidazo[1,2-*a*]pyridin-3-yl)-1-(4-methyl-2-phenylthiazol-5-yl)prop-2-en-1-one (8a). Yellow solid; 89 %; 254–256 °C; IR (cm^{-1}): 1650 (C=O), 1580 (C=C); ^{1}H NMR ($CDCl_3$, 400 MHz): δ = 8.52 (d, *J* = 6.8 Hz, 1H), 8.17 (d, *J* = 15.2 Hz, 1H, CH=CH), 8.00 (dd, *J* = 1.6, 6.8 Hz, 2H), 7.80-7.77 (m, 3H), 7.50-7.43 (m, 4H), 7.27-7.20 (m, 2H), 7.16-7.11 (m, 2H), 2.82 (s, 3H, -CH3); ^{13}C NMR ($CDCl_3$, 75 MHz): δ = 186.27, 169.02, 162.72, 162.23, 145.50, 144.14, 136.10, 133.22, 130.11, 128.94, 128.80, 128.65, 128.43, 127.27, 127.09, 126.34, 122.05, 116.10, 115.49, 114.70, 114.12, 11.22; HRMS: Calcd. for $C_{26}H_{18}FN_3OS$; Exact mass: 439.1155, found (ESI M+H) HRMS: *m*/*z* 440.3810 (M+H).

(2*E*)-1-(2-(4-chlorophenyl)-4-methylthiazol-5-yl)-3-(2-(4-fluorophenyl)-*H*-imidazo[1,2-*a*]pyridin-3-yl)prop-2-en-1-one (8b). Yellow solid; 85 %; 258–260 °C; IR (cm^{-1}): 1651 (C=O), 1576 (C=C); ^{1}H NMR ($CDCl_3$, 400 MHz): δ = 8.51 (d, *J* = 6.8 Hz, 1H), 8.17 (d, *J* = 15.6 Hz, 1H, CH=CH), 7.95-7.91 (m, 3H), 7.79-7.76 (m, 3H), 7.47-7.43 (m, 4H), 7.24 (d, *J* = 8.4 Hz, 1H), 7.18-7.12 (m, 1H), 2.80 (s, 3H, -CH_3); ^{13}C NMR ($CDCl_3$, 75 MHz): δ = 186.84, 169.13, 162.86, 162.12, 145.44, 144.38, 136.17, 134.21, 131.40, 129.93, 129.78, 129.18, 128.91, 128.50, 126.94, 126.32, 122.08, 116.28, 115.33, 114.82, 114.05, 11.42; HRMS: Calcd. for $C_{26}H_{17}ClFN_3OS$; Exact mass: 473.0765, found (ESI M+H) HRMS: *m*/*z* 474.0463 (M+H).

(2*E*)-3-(2-(4-fluorophenyl)-*H*-imidazo[1,2-*a*]pyridin-3-yl)-1-(2-(4-methoxyphenyl)-4-methylthiazol-5-yl)prop-2-en-1-one (8c). Yellow solid; 92 %; 234–238 °C; IR (cm^{-1}): 1645 (C=O), 1567 (C=C); ^{1}H NMR ($CDCl_3$, 400 MHz): δ = 8.60-8.57 (m, 1H), 8.23 (d, *J* = 15.6 Hz, 1H, –CH=CH), 7.99-7.90 (m, 2H), 7.86-7.82 (m, 3H), 7.74-7.55 (m, 2H), 7.18-7.11 (m, 3H), 7.06-6.90 (m, 2H), 3.82 (s, 3H, -OCH_3), 2.67 (s, 3H, -CH_3); ^{13}C NMR ($CDCl_3$, 75 MHz): δ = 186.27, 168.82, 162.53, 162.04, 160.41, 144.90, 144.13, 136.25, 131.00, 129.31, 128.50, 128.00, 127.26, 126.42, 126.08, 122.13, 116.51, 115.11, 114.82, 114.32, 114.03, 55.61, 11.00; HRMS: Calcd. for $C_{27}H_{20}FN_3O_2S$; Exact mass: 469.1260, found (ESI M+H) HRMS: *m*/*z* 470.1581 (M+H).

(2*E*)-1-(4-methyl-2-phenylthiazol-5-yl)-3-(2-*p*-tolyl-*H*-imidazo[1,2-*a*]pyridin-3-yl)prop-2-en-1-one (8d). Yellow solid; 87 %; 208–210 °C; IR (cm^{-1}): 1643 (C=O), 1536 (C=C); ^{1}H NMR ($CDCl_3$, 400 MHz): δ = 8.51 (d, *J* = 6.8 Hz, 1H), 8.21 (d, *J* = 15.6 Hz, 1H, -CH=CH), 7.94 (d, *J* = 6.8 Hz, 2H), 7.80 (d, *J* = 8.8 Hz, 1H), 7.67 (d, *J* = 7.6 Hz, 2H), 7.46-7.41 (m, 3H), 7.35 (d, *J* = 7.6 Hz, 2H), 7.20-7.16 (m, 2H), 7.10-7.08 (m, 1H), 2.78 (s, 3H, -CH_3), 2.46 (s, 3H, -CH_3); ^{13}C NMR ($CDCl_3$, 75 MHz): δ = 186.0, 168.9, 162.2, 145.5, 144.4, 138.4, 136.0, 133.2, 130.7, 130.1, 129.5, 129.4, 128.5, 127.4, 127.1, 127.0, 126.0, 122.1, 115.2, 114.3, 114.0, 24.2, 11.1; HRMS: Calcd. for $C_{27}H_{21}N_3OS$; Exact mass: 435.1405, found (ESI M+H) HRMS: *m*/*z*: 436.1478 (M+H).

(2*E*)-1-(2-(4-chlorophenyl)-4-methylthiazol-5-yl)-3-(2-*p*-tolyl-*H*-imidazo[1,2-a]pyridin-3-yl)prop-2-en-1-one (8e). Yellow solid; 89 %; 210–214 °C; IR (cm^{-1}): 1666 (C=O), 1579 (C=C); ^{1}H NMR ($CDCl_3$, 400 MHz): δ = 8.32 (d, *J* = 8.8 Hz, 1H), 8.20 (d, *J* = 15.6 Hz, 1H, -CH=CH), 7.99-7.79 (m, 3H), 7.77 (d, *J* = 8.0 Hz, 1H), 7.67 (d, *J* = 7.6 Hz, 2H), 7.52-7.43 (m, 2H), 7.40-7.34 (m, 2H), 7.17 (d, *J* = 15.6 Hz, 1H, -CH=CH), 7.11-7.08 (m, 1H), 2.77 (s, 3H, -CH_3), 2.46 (s, 3H, -CH_3); ^{13}C NMR ($CDCl_3$, 75 MHz): δ = 181.91, 167.49, 159.69, 152.84, 147.60, 139.16, 137.18, 131.35, 130.87, 130.41, 129.72, 129.61, 129.38, 129.34, 128.03, 127.28, 118.97, 118.30, 117.89, 117.32, 115.19, 21.42, 18.53; HRMS: Calcd. for $C_{27}H_{20}ClN_3OS$; Exact mass: 469.1016, found (ESI M+H) HRMS: *m*/*z* 470.1101 (M+H).

(2*E*)-1-(2-(4-methoxyphenyl)-4-methylthiazol-5-yl)-3-(2-*p*-tolyl-*H*-imidazo[1,2-*a*]pyridin-3-yl)prop-2-en-1-one (8f). Yellow solid; 90 %; 232–234 °C; IR (cm^{-1}): 1644 (C=O), 1582 (C=C); ^{1}H NMR ($CDCl_3$, 400 MHz): δ = 8.51 (d, *J* = 6.8 Hz, 1H), 8.18 (d, *J* = 15.6 Hz, 1H, -CH=CH), 7.93 (d, *J* = 6.8 Hz, 2H), 7.76 (d, *J* = 8.8 Hz, 1H), 7.67 (d, *J* = 8.0 Hz, 2H), 7.43-7.41 (m, 1H), 7.39-7.34 (m, 2H), 7.27-7.16 (m, 1H), 7.11 (d, *J* = 6.8 Hz, 1H), 6.97 (d, *J* = 8.8 Hz, 2H), 3.88 (s, 3H, -OCH_3), 2.77 (s, 3H, -CH_3), 2.46 (s, 3H, -CH_3); ^{13}C NMR ($CDCl_3$, 75 MHz): δ = 181.97, 169.03, 162.08, 159.81, 152.57, 147.52, 139.07, 130.95, 129.60, 129.47, 129.37, 129.34, 129.27, 128.53, 127.07, 125.77, 125.21, 123.01, 119.55, 118.30, 114.43, 55.49, 21.32, 18.61; HRMS: Calcd. for $C_{28}H_{23}N_3O_2S$; Exact mass: 465.1511, found (ESI M+H) HRMS: 466.1500 (M+H).

(2*E*)-3-(2-(4-chlorophenyl)-6-methyl-*H*-imidazo[1,2-*a*]pyridin-3-yl)-1-(4-methyl-2-phenylthiazol-5-yl)prop-2-en-1-one (8g). Yellow solid; 85 %; 246–250 °C; IR (cm^{-1}): 1647 (C=O), 1562 (C=C); ^{1}H NMR ($CDCl_3$, 400 MHz): δ = 8.27 (s, 1H), 8.11 (d, *J* = 15.4 Hz, 1H, -CH=CH), 8.01-7.99 (m, 2H), 7.88-7.85 (m, 1H), 7.75-7.71 (m, 2H), 7.65 (d, *J* = 8.8 Hz, 1H), 7.53-7.47 (m, 3H), 7.38 (d, *J* = 8.4 Hz, 1H), 7.29-7.27 (m, 1H), 7.13 (d, *J* = 15.2 Hz, 1H, -CH=CH), 2.81 (s, 3H, -CH_3), 2.47 (s, 3H, -CH_3); ^{13}C NMR ($CDCl_3$, 75 MHz): δ = 181.94, 169.14, 159.98, 150.48, 146.49, 135.13, 132.79, 132.65, 131.70,

131.21, 130.71, 130.45, 129.15, 129.12, 128.85, 126.93, 124.44, 122.92, 119.99, 117.81, 117.60, 24.44, 18.62; HRMS: Calcd. for $C_{27}H_{20}ClN_3OS$; Exact mass: 469.1016, found (ESI M+H) HRMS: *m/z* 470.1094 (M+H).

(2*E*)-1-(2-(4-chlorophenyl)-4-methylthiazol-5-yl)-3-(2-(4-chlorophenyl)-6-methyl-*H*-imidazo[1,2-*a*]pyridin-3-yl)prop-2-en-1-one (8h). Yellow solid; 89 %; 254–256 °C; IR (cm^{-1}): 1638 (C=O), 1516 (C=C); ^{1}H NMR ($CDCl_3$, 400 MHz): δ = 8.32 (d, *J* = 6.4 Hz, 1H), 8.26 (s, 1H), 8.12 (d, *J* = 15.6 Hz, 1H, -CH=CH), 7.98 (d, *J* = 6.8 Hz, 1H), 7.96-7.94 (d, *J* = 6.8 Hz, 1H), 7.71 (d, *J* = 6.8 Hz, 1H), 7.67 (d, *J* = 6.8 Hz, 1H), 7.54-7.50 (m, 2H), 7.49-7.44 (m, 2H), 7.30-7.28 (m, 1H), 7.11 (d, *J* = 15.6 Hz, 1H, -CH=CH), 2.79 (s, 3H, -CH_3), 2.48 (s, 3H, -CH_3); ^{13}C NMR ($CDCl_3$, 75 MHz): δ = 185.90, 169.11, 162.08, 145.45, 144.03, 138.56, 136.00, 134.54, 134.29, 134.11, 131.23, 131.17, 129.33, 129.10, 128.91, 128.49, 127.67, 122.09, 114.87, 114.60, 114.09, 24.41, 12.72; HRMS: Calcd. for $C_{27}H_{19}Cl_2N_3OS$; Exact mass: 503.0626, found (ESI M+H) HRMS: *m/z* 504.0717 (M+H).

(2*E*)-3-(2-(4-chlorophenyl)-6-methyl-*H*-imidazo[1,2-*a*]pyridin-3-yl)-1-(2-(4-methoxyphenyl)-4-methylthiazol-5-yl)prop-2-en-1-one (8i). Yellow solid; 90 %; 248–250 °C; IR (cm^{-1}): 1640 (C=O), 1571 (C=C); ^{1}H NMR ($CDCl_3$, 400 MHz): δ = 8.25 (s, 1H), 8.09 (d, *J* = 15.6 Hz, 1H, -CH=CH), 7.95-7.92 (m, 2H), 7.71 (m, *J* = 6.8 Hz, 2H), 7.64 (d, *J* = 8.8 Hz, 1H), 7.52 (d, *J* = 6.8 Hz, 2H), 7.27 (d, *J* = 8.8 Hz, 2H), 7.11 (d, *J* = 15.6 Hz, 1H, -CH=CH), 6.97 (d, *J* = 6.8 Hz, 1H), 3.88 (d, 3H, -OCH_3), 2.78 (s, 3H, -CH_3), 2.46 (s, 3H, -CH_3); ^{13}C NMR ($CDCl_3$, 75 MHz): δ = 181.80, 169.14, 162.14, 160.04, 150.29, 146.43, 135.06, 134.58, 132.72, 130.32, 129.61, 129.12, 128.71, 128.57, 125.79, 124.33, 122.88, 122.15, 120.25, 117.83, 117.58, 55.48, 25.12, 18.62; HRMS: Calcd. for $C_{28}H_{22}ClN_3O_2S$; Exact mass: 499.1121, found (ESI M+H) HRMS: *m/z* 500.1205 (M+H).

4-(6-methyl-3-((*E*)-3-(4-methyl-2-phenylthiazol-5-yl)-3-oxoprop-1-enyl)-*H*-imidazo[1,2-*a*]pyridin-2-yl) benzonitrile (8j). Yellow solid; 84 %; 282–284 °C; IR (cm^{-1}): 3030 (CH), 2226 (CN), 1646 (C=O), 1569 (C=C); ^{1}H NMR ($CDCl_3$, 400 MHz): δ = 8.31 (s, 1H), 8.17 (d, *J* = 15.6 Hz, 1H, -CH=CH), 8.03-7.96 (m, 2H), 7.90-7.83 (m, 2H), 7.72-7.66 (m, 1H), 7.55-7.46 (m, 5H), 7.20 (d, *J* = 15.6 Hz, 1H, -CH=CH), 7.11-7.06 (m, 1H), 2.80 (s, 3H, -CH_3), 2.46 (s, 3H, -CH_3); ^{13}C NMR ($CDCl_3$, 75 MHz): δ = 184.62, 169.11, 161.99, 145.07, 144.45, 137.25, 136.00, 134.23, 133.33, 133.11, 132.42, 129.30, 128.77, 128.29, 127.91, 127.56, 124.09, 122.23, 115.80, 114.98, 114.58, 114.04, 112.05, 12.06; HRMS: Calcd. for $C_{28}H_{20}N_4OS$; Exact mass: 460.1358, found (ESI M+H) HRMS: *m/z* 461.1435 (M+H).

4-(3-((*E*)-3-(2-(4-chlorophenyl)-4-methylthiazol-5-yl)-3-oxoprop-1-enyl)-6-methyl-*H*-imidazo[1,2-*a*]pyridin-2-yl)benzonitrile (8k). Yellow solid; 88 %; 250–254 °C; IR (cm^{-1}): 3031 (CH), 2225 (CN), 1640 (C=O), 1577 (C=C); ^{1}H NMR ($CDCl_3$, 400 MHz): δ = 8.12 (d, *J* = 15.6 Hz, 1H, -CH=CH), 8.01 (d, *J* = 6.4 Hz, 1H), 7.99-7.96 (m, 2H), 7.94 (d, *J* = 6.8 Hz, 2H), 7.84 (d, *J* = 6.8 Hz, 2H), 7.68 (d, *J* = 8.8 Hz, 1H), 7.52-7.46 (m, 2H), 7.33-7.30 (m, 1H), 7.16 (d, *J* = 15.6 Hz, 1H, -CH=CH), 2.84 (s, 3H -CH_3), 2.49 (s, 3H, -CH_3); ^{13}C NMR ($CDCl_3$, 75 MHz): δ = 185.43, 169.24, 162.00, 145.13, 144.52, 137.11, 136.05, 134.43, 134.03, 133.09, 132.54, 131.20, 129.47, 128.87, 128.11, 127.66, 122.09, 115.14, 114.88, 114.18, 114.00, 112.11, 24.43, 12.34; HRMS: Calcd. for $C_{28}H_{19}ClN_4OS$; Exact mass: 494.0968, found (ESI M+H) HRMS: *m/z* 495.1043 (M+H).

4-(3-((*E*)-3-(2-(4-methoxyphenyl)-4-methylthiazol-5-yl)-3-oxoprop-1-enyl)-6-methyl-*H*-imidazo[1,2-*a*]pyridin-2-yl)benzonitrile (8l). Yellow solid; 89 %; 248–250 °C; IR (cm^{-1}): 2835 (CH), 2227 (CN), 1672 (C=O), 1568 (C=C); ^{1}H NMR ($CDCl_3$, 400 MHz): δ = 8.39 (m, 1H), 8.19 (d, *J* = 15.6 Hz, 1H, -CH=CH), 8.00-7.91 (m, 2H), 7.75-7.68 (m, 2H), 7.61-7.57 (m, 1H), 7.50-7.42 (m, 2H), 7.25-7.19 (m, 2H), 7.09 (d, *J* = 15.6 Hz, 1H, -CH=CH), 7.00-6.94 (m, 1H), 3.80 (s, 3H, -OCH_3), 2.72 (s, 3H, -CH_3), 2.39 (s, 3H, -CH_3); ^{13}C NMR ($CDCl_3$, 75 MHz): δ = 183.56, 168.56, 162.44, 160.32, 145.76, 144.41, 137.25, 136.35, 134.22, 133.11, 132.09, 128.90, 128.67, 127.23, 125.09, 122.76, 115.66, 114.46, 114.29, 114.11, 114.01, 112.22, 55.09, 24.07, 12.67; HRMS: Calcd. for $C_{29}H_{22}N_4O_2S$; Exact mass: 490.1463, found (ESI M+H) HRMS: *m/z* 491.5700 (M+H).

PROCEDURE OF THE SRB-ASSAY FOR ANTICANCER SCREENING

Human breast cancer cell line MCF-7 (Source: NCI, USA and NCCS, Pune) was cultured in tissue culture flasks using RPMI-1640 growth medium supplemented with 2 mM glutamine (pH 7.4), 10 % fetal calf serum, 100 µg/mL streptomycin, and 100 units/mL penicillin. The cells were maintained at 37 °C in a CO_2 incubator under an atmosphere of 5 % CO_2 and 95 % relative humidity. At the sub-confluent stage, cells were harvested by treatment with trypsin (0.05 % in PBS containing 0.02 % EDTA) and resuspended in fresh growth medium. Cells exhibiting more than 97 % viability, as determined by trypan blue exclusion, were used for cytotoxicity studies. An aliquot of 100 µL containing approximately 5×10^3 cells/well was seeded into a 96-well tissue culture plate. The cells were allowed to adhere and grow for 24 h at 37 °C in a CO_2 incubator. Test compounds at various concentrations were then added to the wells, and incubation was continued for an additional 48 hours under the same conditions. Suitable blanks and positive controls were included, and all experiments were performed in triplicate. After incubation, cell growth was terminated by gently adding 50 µL of 50 % trichloroacetic acid (TCA) to each well. The plates were incubated at 4 °C

for 1 h to fix the cells. The liquid contents were then carefully removed, and the wells were washed five times with double-distilled water to remove residual TCA and medium. The plates were air-dried completely. Each well was subsequently stained with 100 µL of 0.4 % SRB (sulforhodamine B) solution prepared in 1 % acetic acid, and the plates were incubated at room temperature for 30 minutes. Unbound dye was removed by washing the wells five times with 1 % acetic acid, followed by air drying. Bound dye was solubilized by adding 100 µL of 0.01 M Tris buffer (pH 10.4) to each well, and the plates were gently shaken for 5 minutes on a mechanical shaker. The optical density (OD) was measured at 540 nm using an ELISA plate reader. Cell growth in untreated control wells was considered 100 %, and the percentage of growth inhibition for each test sample was calculated accordingly. The GI_{50} values (concentration causing 50 % growth inhibition) were determined by regression analysis.

DISC DIFFUSION METHOD

Inocula of each bacterial and fungal pathogen were prepared by culturing them overnight in nutrient broth at 37 °C. The resulting broth cultures were used for further studies. Bacterial suspensions were adjusted with sterile saline to match the turbidity of the 0.5 McFarland standard. Nutrient agar plates were then inoculated with 200 µL of the diluted microbial suspension, and the cultures were evenly spread across the agar surface using sterile cotton swabs. Antibiotic discs were aseptically placed on the inoculated agar surface using sterile forceps.

All synthesized compounds were dissolved in dimethyl sulfoxide (DMSO) to obtain a final concentration of 2 mg/mL. A 100 µL aliquot of each compound solution was applied to sterile discs. A control disc containing 100 µL of DMSO alone was included to evaluate any intrinsic antimicrobial effect of the solvent. The plates were incubated at 37 °C for 24 h. Fluconazole and ciprofloxacin served as standard reference drugs for antifungal and antibacterial activity, respectively. Following incubation, the antimicrobial efficacy of the synthesized compounds was assessed by measuring the diameter of the zone of inhibition around each disc, which reflected the extent of microbial growth inhibition.

RESULTS AND DISCUSSION

Chemistry

In the present study, a novel series of imidazo[1,2-*a*]pyridine-integrated thiazole chalcones (**8a-l**) were synthesized via Claisen–Schmidt condensation of substituted thiazolyl ketones (**3a-c**) with substituted imidazo[1,2-*a*]pyridine-3-carbaldehydes (**7a-d**) in ethanol, using 10 % aqueous sodium hydroxide as a base (Scheme 1). The starting thiazolyl ketones (**3a-c**) were prepared in good yields by refluxing substituted thiobenzamides (**1**) with 3-chloro-2,4-pentanedione (**2**) in the presence of sodium hydroxide, following a literature-reported method with minor modifications.[30] The crude products were purified by column chromatography on silica gel (100–200 mesh) using 10 % ethyl acetate in hexane as the eluent. The imidazo[1,2-*a*]pyridine-3-carbaldehydes (**7a-d**) were obtained in good yields via the Vilsmeier–Haack reaction of imidazo[1,2-*a*]pyridines (**6a-d**) with phosphorus oxychloride in the presence of dimethylformamide.[31] The

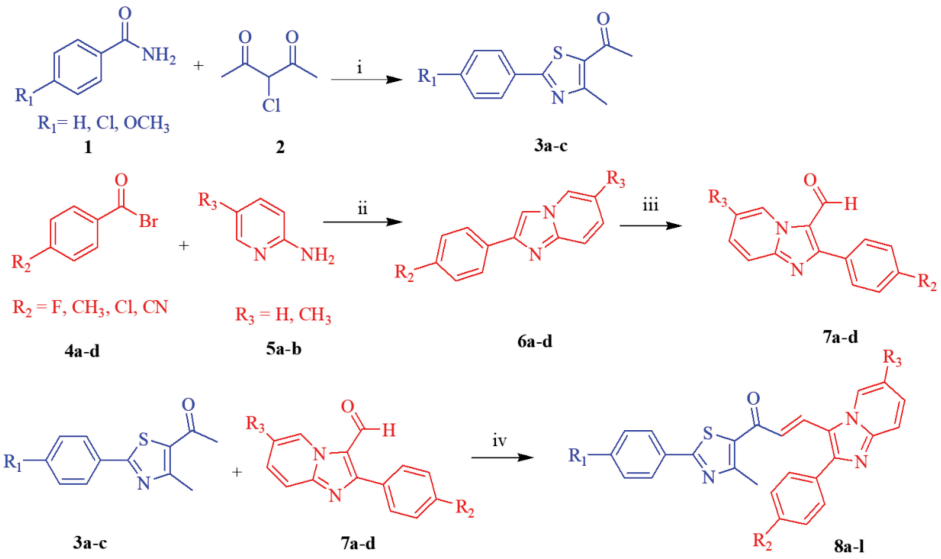

Scheme 1. Reagents and conditions: (i) NaOH, ethanol, reflux, 7-8 h (ii) ethanol, reflux, 7-8 h (iii) DMF, $POCl_3$, 0–5 °C, 8 h (iv) 10 % NaOH, ethanol, 24 h at RT.

structures of all the synthesized compounds were confirmed by FT-IR, ^{1}H NMR, ^{13}C NMR, and HRMS spectroscopic analyses. The *α,β*-unsaturated system in chalcones typically shows a large coupling constant (J ≈ 15–16 Hz) between the olefinic protons (Hα and Hβ), which is characteristic of the *E*-configuration**.** All synthesized hybrids exhibited this diagnostic *trans*-coupling value.

Biological Evaluation

IN VITRO ANTICANCER ACTIVITY

The synthesized novel imidazo[1,2-*a*]pyridine-integrated thiazole chalcones **(8a-l)** were evaluated for their *in vitro* anticancer potential against the human breast cancer cell line MCF-7 using the sulforhodamine B (SRB) assay method.[32] The MCF-7 cell line was selected as the primary screening model because it represents a well-established estrogen-receptor–positive breast cancer system and is widely used for preliminary cytotoxicity assessment of chalcone- and imidazo[1,2-*a*]pyridine-based scaffolds. Moreover, previous reports [23,33] have demonstrated that these structural classes exhibit preferential activity toward MCF-7 cells, making this model particularly relevant for initial biological evaluation. During the screening process, three parameters such as GI_{50}, TGI, and LC_{50} were determined, and the results are presented in Table 1.

The GI_{50} value (growth inhibitory concentration) denotes the concentration of the compound that reduces cellular growth by 50 % relative to untreated control cells. The TGI (total growth inhibition) and LC_{50} (lethal concentration) values represent the concentrations required for complete growth arrest and for inducing 50 % cell death, respectively. Based on GI_{50} values, the compounds were categorized according to their cytotoxic potential as follows: inactive (>100 µM), moderately active (>10 – <100 µM), and highly active (<10 µM).

The majority of the synthesized imidazo[1,2-*a*]-pyridine–thiazole–chalcone derivatives (**8a–l**) exhibited moderate *in vitro* anticancer activity against the human breast cancer cell line MCF-7 (estrogen receptor-positive). Among the tested compounds, **8i** displayed the most potent growth inhibitory effect with a GI_{50} value of 19.0 µM, while compounds **8f**, **8e**, and **8b** showed moderate activity with GI_{50} values of 83.0, 92.0, and 95.0 µM, respectively. These findings indicate that several synthesized chalcones possess good to moderate cytotoxic activity, comparable to that of the reference drug Adriamycin (ADR) (GI_{50} = 0.4 µM). In contrast, the remaining imidazo[1,2-*a*]-pyridine–thiazole–chalcones exhibited negligible inhibitory effects against MCF-7 cells, with GI_{50} values exceeding 100 µM.

Furthermore, comparative evaluation of TGI (total growth inhibition) and LC_{50} (lethal concentration for 50 % cell death) values relative to adriamycin revealed that all synthesized compounds (**8a–l**) were inactive, with TGI and LC_{50} values greater than 100 µM.

Overall, these results suggest that certain imidazo[1,2-*a*]pyridine–thiazole–chalcone derivatives exhibit promising anticancer potential and merit further investigation for structural optimization and therapeutic development.

The structure–activity relationship (SAR) analysis of the synthesized imidazo[1,2-*a*]pyridine–thiazole–chalcones (**8a–l**) revealed that the electronic nature and position of substituents on both the thiazole and imidazo[1,2-*a*]pyridine rings significantly influence anticancer activity against MCF-7 cells. In particular, the presence of electron-donating substituents such as the methoxy group (-OCH_3) at the para-position of the phenyl ring attached to the thiazole moiety significantly enhances anticancer activity. This enhancement is attributed to increased electron

Table 1. *In vitro* anticancer screening of imidazo[1,2-*a*] pyridine-integrated thiazole chalcones **(8a-l)** against human breast cancer cell line MCF-7[a].

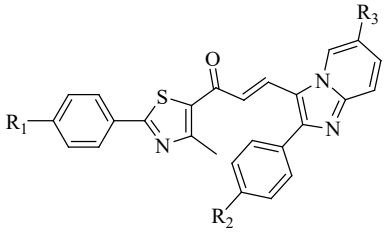

Compounds	MCF-7					
	R_1	R_2	R_3	LC_{50}[b]	TGI[c]	GI_{50}[d]
8a	-H	-F	-H	>100	>100	>100
8b	-Cl	-F	-H	>100	>100	95.0
8c	-OCH_3	-F	-H	>100	>100	>100
8d	-H	-CH_3	-H	>100	>100	>100
8e	-Cl	-CH_3	-H	>100	>100	92.0
8f	-OCH_3	-CH_3	-H	>100	>100	83.0
8g	-H	-Cl	-CH_3	>100	>100	>100
8h	-Cl	-Cl	-CH_3	>100	>100	>100
8i	-OCH_3	-Cl	-CH_3	>100	>100	19.0
8j	-H	-CN	-CH_3	>100	>100	>100
8k	-Cl	-CN	-CH_3	>100	>100	>100
8l	-OCH_3	-CN	-CH_3	>100	>100	>100
ADR				>100	10.0	0.4

[a] Concentrations in µM; [b] Concentration of drug resulting in a 50 % reduction in the measured protein at the end of the drug treatment as compared to that at the beginning) calculated from [(*Ti* – *Tz*) / *Tz*] × 100 = –50; [c] Drug concentration resulting in total growth inhibition (TGI) will calculated from Ti = Tz; d Growth inhibition of 50 % (GI_{50}) calculated from [(*Ti* – *Tz*) / (*C* – *Tz*)] × 100 = 50.

density on the aromatic ring, which may facilitate improved π–π stacking or hydrogen bonding interactions with biological targets involved in cancer cell proliferation. Similarly, the introduction of electron-donating groups on the imidazo[1,2-*a*]pyridine scaffold further contributes to improved cytotoxic potency, suggesting that these substituents favorably influence the electronic environment and molecular recognition properties of the chalcone framework. Among the tested derivatives, compound **8i** demonstrated the most potent activity (GI_{50} = 19.0 μM) against MCF-7 cells. This compound features a methoxy (-OCH_3) group at the para-position of the phenyl ring in the thiazole moiety and a chloro (-Cl) substituent on the imidazo[1,2-*a*]pyridine nucleus. The synergistic electronic and steric effects of these substituents likely contribute to its superior biological performance. Although most compounds showed weak or no antiproliferative activity, the moderate potency of **8i** is consistent with structurally related chalcone-, thiazole-, and imidazo[1,2-*a*]pyridine-based hybrids reported in the literature,[33,34] which commonly exhibit cytotoxicity in the low-to-mid μM range.

In contrast, compound **8l**, bearing a methoxy (-OCH_3) group at the para-position of the thiazole phenyl ring but a cyano (-CN) group – an electron-withdrawing substituent – on the imidazo[1,2-*a*]pyridine moiety, exhibited negligible anticancer activity (GI_{50} > 100 μM). The diminished activity may be attributed to the decreased electron density and altered molecular polarity induced by the electron-withdrawing group, which could adversely affect the compound's ability to interact with cellular targets. Overall, electron-donating substituents enhance, while electron-withdrawing groups reduce, the anticancer potential of these chalcone hybrids, providing useful guidance for future structural optimization.

Furthermore, to strengthen the biological interpretation, a discussion of possible mechanisms of action has been incorporated. Literature reports[33–37] suggest that chalcone- and imidazo[1,2-*a*]pyridine-based derivatives may act by inducing apoptosis through ROS generation, disrupting mitochondrial membrane potential, or inhibiting tubulin polymerization. Although detailed mechanistic studies were not conducted in the present work, these established pathways offer a plausible explanation for the observed cytotoxic effects and provide direction for future investigations.

ANTIMICROBIAL ACTIVITY

The synthesized novel imidazo[1,2-*a*]pyridine–thiazole–chalcone derivatives (**8a–l**) were evaluated for their *in vitro* antimicrobial activity using the disc diffusion method, as reported in the literature. The antimicrobial efficacy was determined by measuring the diameter of the zone of inhibition (mm). The compounds were tested against Gram-positive bacteria (*Staphylococcus aureus*, *Bacillus subtilis*) and Gram-negative bacteria (*Escherichia coli*, *Pseudomonas aeruginosa*). Dimethyl sulfoxide (DMSO) was used as the solvent control, and the results are summarized in Table 2.

Among the tested compounds, **8g**, **8j**, **8k**, and **8d** exhibited zones of inhibition of 26, 25, and 24 mm, respectively, against *Staphylococcus aureus* (ATCC 6538), demonstrating antibacterial activity comparable to the standard drug ciprofloxacin (26 mm). Compounds **8e**, **8j**, and **8l** showed zones of inhibition of 26 and 25 mm, respectively, against *Bacillus subtilis* (ATCC 6633), also comparable to ciprofloxacin (30 mm).

Against *Pseudomonas aeruginosa* (ATCC 9027), compounds **8l**, **8c**, and **8j** displayed notable antibacterial activity with inhibition zones of 28, 27, and 26 mm, respectively, comparable to ciprofloxacin (28 mm). Similarly, compounds **8a**, **8h**, and **8g** exhibited 26 and 25 mm zones of inhibition against *Escherichia coli* (ATCC 8739), showing antibacterial activity similar to ciprofloxacin (32 mm). All synthesized derivatives exhibited moderate inhibitory activity against the fungal strain *Candida albicans* (ATCC 10231), with inhibition zones comparable to ciprofloxacin (32 mm).

Overall, several compounds demonstrated good to moderate antimicrobial activity (Figure 2). These findings indicate that imidazo[1,2-*a*]pyridine–thiazole–chalcone hybrids represent a promising class of antimicrobial agents, meriting further exploration for potential therapeutic development.

Table 2. Antimicrobial activity of imidazo[1,2-*a*]pyridine-integrated thiazole chalcones (**8a-l**).

Compound	Zone of inhibition in mm												
	8a	8b	8c	8d	8e	8f	8g	8h	8i	8j	8k	8l	Ciprofloxacin
B. subtilis	22	24	18	23	26	19	13	18	24	26	22	25	30
S. aureus	20	23	17	24	23	21	26	18	19	25	24	22	26
E. coli	26	24	21	18	20	22	25	26	24	21	16	19	32
P. aerugenosa	25	23	27	21	22	20	22	24	16	26	24	28	31
C. albicans	21	17	18	12	18	16	19	20	22	23	21	20	28

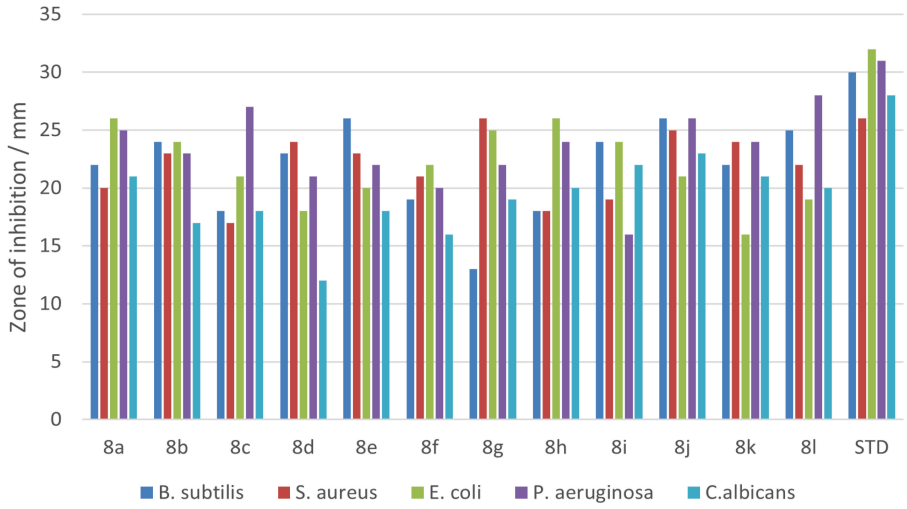

Figure 2. Antimicrobial activity of imidazo[1,2-*a*]pyridine-integrated thiazole chalcones (**8a-l**).

Supplementary Information. Supporting information to the paper is attached to the electronic version of the article at: https://doi.org/10.5562/cca4224.

PDF files with attached documents are best viewed with Adobe Acrobat Reader which is free and can be downloaded from Adobe's web site.

CONCLUSION

In conclusion, a novel series of imidazo[1,2-*a*]pyridine–thiazole–chalcone derivatives (**8a–l**) were synthesized and evaluated for their *in vitro* anticancer and antimicrobial activities. Several compounds exhibited moderate anticancer potential against MCF-7 cells, with compound **8i** showing the highest potency (GI_{50} = 19.0 µM). The SAR analysis revealed that electron-donating substituents enhance, while electron-withdrawing groups reduce, cytotoxic activity. Moreover, many derivatives displayed broad-spectrum antimicrobial activity comparable to ciprofloxacin. These findings highlight imidazo[1,2-*a*] pyridine–thiazole–chalcones as promising scaffolds for the development of new anticancer and antimicrobial agents.

Acknowledgment. The authors express their sincere gratitude to the Tata Memorial Centre, Advanced Centre for Treatment, Research and Education in Cancer (ACTREC), Kharghar, Navi Mumbai–410210, for conducting the *in vitro* anticancer screening.

REFERENCES

[1] H. Sung, J. Ferlay, R. L. Siegel, M. Laversanne, I. Soerjomataram, A. Jemal, F. Bray, *CA-Cancer J. Clin.* **2021**, *71*, 209–249. https://doi.org/10.3322/caac.21660

[2] F. Bray, M. Laversanne, H. Sung, J. Ferlay, R. L. Siegel, I. Soerjomataram, A. Jemal, *CA-Cancer J. Clin*. **2024**, *74*, 229–263. https://doi.org/10.3322/caac.21834

[3] N. Harbeck, F. P. Llorca, J. Cortes, M. Gnant, N. Houssami, P. Poortmans, K. Ruddy, J. Tsang, F. Cardoso, *Nat. Rev. Dis. Primers*, **2019**, *5*, 66. https://doi.org/10.1038/s41572-019-0111-2

[4] F. Bray, J. Ferlay, I. Soerjomataram, R. L. Siegel, L. A. Torre, A. Jemal, *CA-Cancer J. Clin.* **2018**, *68*, 394–424. https://doi.org/10.3322/caac.21492

[5] E. Marchesi, D. Perrone, M. L. Navacchia, *Pharmaceutics* **2023**, *15*, 2185. https://doi.org/10.3390/pharmaceutics15092185

[6] A. K. Bagdi, S. Santra, K. Monir, A. Hajra, *Chem Commun.* **2015**, *51*, 1555–1575. https://doi.org/10.1039/C4CC08495K

[7] R. Goel, V. Luxami, K. Paul, Curr Top Med Chem. 2016, 16, 3590-3616. https://doi.org/10.2174/1568026616666160414122644

[8] A. T. Baviskar, C. Madaan, R. Preet, P. Mohapatra, V. Jain, A. Agarwal, S. K. Guchhait, C. N. Kundu, U. C. Banerjee, P. V. Bharatam, *J Med Chem.* **2011**, *54*, 5013–503. https://doi.org/10.1021/jm200235u

[9] M. Russo, K. Kang, A. Cristofano, *Thyroid*. **2013**, *23*, 1284–1293. https://doi.org/10.1089/thy.2013.0037

[10] M. R. Gangireddy, M. Mantipally, R. Gundla, V. N. Badavath, K. Paidikondala, A. Yamala, *Chemistry Select*. **2019**, *4*, 13622–13629. https://doi.org/10.1002/slct.201902955

[11] T. Liu, X. Peng, Y. Ma, Y. Ji, D. Chen, M. Zheng, D. Zhao, M. Cheng, M. Geng, J. Shen, J. Ai, B. Xiong, *Acta Pharmacol Sin*. **2016**, *37*, 698–707. https://doi.org/10.1038/aps.2016.11

[12] J. Ye, Q. Liu, C. Wang, Q. Meng, H. Sun, J. Peng, X. Ma, K. Liu, *Pharmacol. Rep.* **2013**, 65, 505–512.
[13] B. Rahmutulla, K. Matsushita, M. Satoh, M. Seimiya, S. Tsuchida, S. Kubo, H. Shimada, M. Ohtsuka, M. Miyazaki, F. Nomura, *Oncotarget.* **2014**, *15*, 2404–2417. https://doi.org/10.18632/oncotarget.1650
[14] J. J. Choi, M. W. McCarthy, *Expert Opin. Investig. Drugs*. **2018,** *27*, 193–197. https://doi.org/10.1080/13543784.2018.1426745
[15] T. Aoki, H. Yoshizawa, K. Yamawaki, K. Yokoo, J. Sato, S. Hisakawa, Y. Hasegawa, H. Kusano, M. Sano, H. Sugimoto, Y. Nishitani, T. Sato, M. Tsuji, R. Nakamura, T. Nishikawa, Y. Yamano, *Eur. J. Med. Chem.* **2018**, *155*, 847–868. https://doi.org/10.1016/j.ejmech.2018.06.014
[16] S. Portsmouth, D. van Veenhuyzen, R. Echols, M. Machida, J. C. A. Ferreira, M. Ariyasu, P. Tenke P, T. D. Nagata, *Lancet Infect. Dis.* **2018**, *18*, 1319–1328. https://doi.org/10.1016/S1473-3099(18)30554-1
[17] M. Ghoncheh, Z. Pournamdar, H. Salehiniya, *Asian Pac. J. Cancer Prev.* **2016**, *17*, 43–46. https://doi.org/10.7314/apjcp.2016.17.s3.43
[18] C. Mishra, S. Kumari, M. Tiwari, *Eur. J. Med. Chem.* **2015**, *92*, 1–34. https://doi.org/10.1016/j.ejmech.2014.12.031
[19] P. Bhale, H. Chavan, S. Dongare, S. Shringare, Y. Mule, P. Choudhari, B. Bandgar, *Curr. Bioact. Compd.* **2018**, *14*, 299–308. https://doi.org/10.2174/1573407213666170428112855
[20] P. Bhale, H. Chavan, S. Dongare, S. Shringare, Y. Mule, S. Nagane, B. Bandgar, *Bioorg. Med. Chem. Lett.* **2017**, *27*, 1502–1507. https://doi.org/10.1016/j.bmcl.2017.02.052
[21] S. Dongare, B. Bandgar, P. Bhale, S. Shringare, H. Chavan, *Croat. Chem. Acta* **2019**, *92*, 1–9. https://doi.org/10.5562/cca3418
[22] P. Bhale, H. Chavan, S. Dongare, S. Sankpal, B. Bandgar, *Anti-Cancer Agents Med. Chem.* **2018**, *18*, 757–764. https://doi.org/10.2174/1871520617666170912124258
[23] P. Bhale, S. Shringare, A. Khade, H. Chavan, *Anti-Cancer Agents Med. Chem.* **2021**, *21*, 2216–2223. https://doi.org/10.2174/1871520621666210201095030
[24] S. Shringare, P. Bhale, H. Chavan, P. Hundekari, M. Kulkarni, *Croat. Chem. Acta* **2021**, *94*, 191–199. https://doi.org/10.5562/cca3859
[25] S. Dongare, H. Chavan, D. Surwase, P. Bhale, Y. Mule, B. Bandgar, *J. Chin. Chem. Soc.* **2016**, *63*, 323–330. https://doi.org/10.1002/jccs.201500540
[26] P. Bhale, H. Chavan, S. Shringare, V. Khedkar, R. Tigote, N. Mali, T. Jadhav, N. Kamble, S. Kolat, B. Bandgar, H. Patil, *Synth. Commun.* 2022, *52*, 733–744. https://doi.org/10.1080/00397911.2022.2048860
[27] S. Shringare, H. Chavan, N. Kamble, R. Tigote, P. Bhale, M. Mali, S. Kadam, K. Kadam, G. Pandhare, A. Khalifa, N. Pendpale, M. Kulkarni, B. Bandgar, *Polycycl Aromat Comp.* **2024**, *44*, 5983–5999. https://doi.org/10.1080/10406638.2023.2271113
[28] P. Bhale, H. Chavan, R. Endait, A. Kadam, R. Bopalkar, M. Gaikwad, *Croat. Chem. Acta* **2021**, *94*, 35–41. https://doi.org/10.5562/cca3758
[29] D. Sirsat, P. Bhale, H. Chavan, S. Karape, M. Bachute, *Rasayan Journal of Chemistry* **2020**, *13*, 1589–1597. http://dx.doi.org/10.31788/ RJC.2020.1335768
[30] H. Alharbi, O. Alsalmi, A. I. Alalawy, A. F. Qarah, Abdulrahman A. Alsimaree, A. M. Alqahtani, A. Alsoliemy, N. M. El-Metwaly, *J. Saudi Chem. Soc.* **2024**, *28*, 101800. https://doi.org/10.1016/j.jscs.2023.101800
[31] P. N. James, H. R. Snyder, *Org. Synth.* **1963**, *4*, 539. https://doi.org/10.15227/orgsyn.043.0058
[32] P. Skehan, R. Strong, D. Scadiaro, A. Monks, J. Mc-Mahon, D. Vistica, J. Warren, H. Bokesch, S. Kenney, M. Boyed, *J. Natl. Cancer Inst.* **1990**, *82*, 1107–1112. https://doi.org/10.1093/jnci/82.13.1107
[33] P. Sri Ramya, L. Guntuku, S. Angapelly, C. Digwal, U. Lakshmi, D. Sigalapalli, B. Babu, V. Naidu, A. Kamal, *Eur. J. Med. Chem*. **2018**, *143*, 216–231. https://doi.org/10.1016/j.ejmech.2017.11.010
[34] A. Altaher, M. Adris, S. Aliwaini, A. Awadallah, R. Morjan, *Asian Pac J Cancer Prev.* **2022**, *23*, 2943–2951. https://doi.org/10.31557/APJCP.2022.23.9.2943
[35] R. Gopathi, M. Kumar, G. Kumar, N. Syamprasad, B. Kodiripaka, V. Naidu, B. Babu, *RSC Med. Chem.* **2025**, *16*, 1188–1198. https://doi.org/10.1039/D4MD00838C
[36] W. Liu, M. He, Y. Li, Z. Peng, G. Wang, *J Enzyme Inhib Med Chem.* **2021**, *37*, 9–38. https://doi.org/10.1080/14756366.2021.1976772
[37] J. Moreira, J. Almeida, L. Saraiva, H. Cidade, M. Pinto, *Molecules* **2021**, *26*, 3737. https://doi.org/10.3390/molecules26123737